Wolters Kluwer Health | OvidSP

Main Search Page | Display Knowledge Base | Help | Logoff

Save Article Text | Email Article Text | Print Preview

Full Text

Lippincott Williams & Wilkins

Pharmacogenetics

- This journal has ceased publication.
- Articles are no longer accepted for this title.
- Succeeded by: Pharmacogenetics and Genomics (ISSN: 1744-6872)

Structural heterogeneity at the UDP-glucuronosyltransferase 1 locus: functional consequences of three novel missense mutations in the human *UGT1A7* gene

Author(s): Guillemette, Chantal[a]; Ritter, Joseph K.[b]; Auyeung, Diana J.[b]; Kessler, Fay K.[b]; Housman, David E.[a]

Issue: Volume 10(7), October 2000, pp 629-644

Publication Type: [Original Articles]

Publisher: © 2000 Lippincott Williams & Wilkins, Inc.

Institution(s): [a]Department of Biology and Center for Cancer Research, Massachusetts Institute of Technology, Cambridge, MA and [b]Department of Pharmacology and Toxicology, Virginia Commonwealth University, Richmond, VA, USA

Received 29 January 2000; accepted 22 March 2000

Correspondence to Chantal Guillemette, Laval University, Faculty of Pharmacy and Oncology and Molecular Endocrinology Research Centre, Laval University Medical Centre (CHUL), 2705 Boul. Laurier, T3–67, Ste-Foy, Quebec G1V 4G2, Canada E-mail: chantal.guillemette@crchul.ulaval.ca

ISSN: 0960-314X

Accession: 00008571-200010000-00006

Full Text (PDF) 1949 K

Email Jumpstart

Find Citing Articles

« Table of Contents

About this Journal »

Keywords: glucuronidation, drug metabolism, genetic polymorphism, UGT1A7, benzopyrene

Table of Contents:

« Relation between inducibility of CYP1A1, GSTM1 and lung cancer in a French population.

» Glutathione transferase T1 phenotype affects the toxicokinetics of inhaled methyl chloride in human volunteers.

Links

Abstract

Complete Reference

ArticleLinker

Abstract

One of the most important mechanisms involved in host defense against xenobiotic chemicals and endogenous toxins is the glucuronidation catalysed by UDP-glucuronosyltransferase enzymes (UGT). The role of genetic factors in determining variable rates of glucuronidation is not well understood, but

Outline

- **Abstract**
- **Introduction**
- **Materials and methods**
 - **Subjects**
 - **Polymorphism detection**
 - **Direct sequencing and confirmation of polymorphism**
 - **Genotyping**
 - **Stable expression of human UGT1A7 alleles**
 - **Immunoblot blot analysis of UGT1A7**
 - **Functional UGT enzyme assays**
 - **Expression analysis of UGT1A7**
 - **Statistical analysis**
- **Results**
 - **Identification of three missense mutations in the human UGT1A7 gene**
 - **Presence of four distinct UGT1A7 alleles and their distribution in the population**
 - **Function of the UGT1A7 protein is affected by the newly found polymorphisms**
 - **Expression analysis of UGT1A7**
- **Discussion**
- **Acknowledgements**
- **References**

Graphics

- **Table 1**
- **Fig. 1**
- **Table 2**
- **Fig. 2**
- **Table 3**
- **Fig. 3**
- **Fig. 4**
- **Fig. 5**
- **Table 4**
- **Fig. 6**
- **Table 5**
- **Fig. 7**
- **Fig. 8**

phenotypic evidence in support of such variation has been reported. In the present study, six single nucleotide polymorphisms were discovered in the first exon of the *UGT1A7* gene, which codes for the putative substrate-binding domain, revealing a high structural heterogeneity at the *UGT1* gene locus. The new UGT1A7 proteins differ in their primary structure at amino acid positions 129, 131 and 208, creating four distinct UGT1A7 allelic variants in the human population: *UGT1A7*1* ($N^{129}R^{131}W^{208}$), **2* ($K^{129}K^{131}W^{208}$), **3* ($K^{129}K^{131}R^{208}$), and **4* ($N^{129}R^{131}R^{208}$). In functional studies, HEK cells stably transfected to express the four allelic UGT1A7 variants exhibited significant differences in catalytic activity towards 3-, 7-, and 9-hydroxy-benzo(a)pyrene. *UGT1A7*3* exhibited a 5.8-fold lower relative V_{max} compared to wild-type **1*, whereas **2* and **4* had a 2.6- and 2.8-fold lower relative V_{max} than **1*, respectively, suggesting that these mutations confer slow glucuronidation phenotype. Kinetic characterization suggested that these differences were primarily attributable to altered V_{max}. Additionally, it suggested that each amino acid substitutions can independently affect the UGT1A7 catalytic activity, and that their effects are additive. The expression pattern of UGT1A7 studied herein and its catalytic activity profile suggest a possible role of UGT1A7 in the detoxification and elimination of carcinogenic products in lung. A population study demonstrated that a considerable proportion of the population (15.3%) was found homozygous for the low activity allele containing all three missense mutations, *UGT1A7*3*. These findings suggest that further studies are needed to investigate the impact of the low UGT1A7 conjugator genotype on individual susceptibility to chemical-induced diseases and responses to therapeutic drugs.

Introduction

Recent evidence supports the concept that polymorphic variations in genes encoding drug metabolism enzymes (DMEs) are likely to play an important role in disease susceptibility and clinical response to therapeutic drugs (Ingelman-Sundberg, 1998;Aithal et al., 1999;Nebert et al., 1999). An increasing number of variants have been described for most of the genes that code for the phase I and II DMEs. However, the glucuronidation pathway, one of the most important phase II conjugative pathways, has been poorly investigated with regard to genetic polymorphisms, although marked inter-individual variation in glucuronidation of several compounds has been observed in humans.

Glucuronidation, catalysed by the superfamily of UDP-glucuronosyltransferase enzymes (UGTs), results in the detoxification and enhanced elimination of a large number of chemical compounds, including endogenous and exogenous molecules (Dutton, 1980). Therefore, glucuronidation represents a major chemical defense pathway, where many of the substances primarily inactivated and eliminated by UGT enzymes, including carcinogenic drugs, environmental pollutants, and endogenous toxins, contribute to human carcinogenesis. In addition, this enzymatic system is clearly involved in the homeostasis of steroid and thyroid hormones as well as bile acids (Ritter et al., 1992a;Pillot et al., 1993;Bélanger et al., 1998;Hum et al., 1999). The importance of this biochemical pathway in humans is supported by the existence of genetic defects and polymorphisms affecting individual UGT activities, which have a profound impact on the health of affected individuals. In particular, genetic

variability leading to an inactive allele in the *UGT1A1* locus is shown to have potentially lethal effects, as seen in the familial forms of the unconjugated hyperbilirubinemia disorder, Crigler–Najjar type I and II (Bosma et al., 1992;Ritter et al., 1993). To date, two UGT gene subfamilies have been identified in humans, UGT1 and UGT2 (Mackenzie et al., 1997). In contrast to the UGT2B family, which is comprised of several genes, the entire UGT1 family is derived from a single gene locus (*UGT1*) coding for nine functional proteins (UGT1A1, UGT1A3–UGT1A10) and three pseudogenes (UGT1A2, UGT1A11–UGT1A12) (Ritter et al., 1992b;Owens & Ritter, 1995). The mechanism underlying the existence of 12 UGT1A transcripts resides in the presence of 12 alternative exons 1, which confer the substrate specificity, shared with four common exons coding for the cosubstrate binding domain.

The presence of polymorphisms in the glucuronic acid conjugation pathway is primarily suggested at the phenotypic level with wide inter-individual variations in the glucuronidation of steroids and drugs. Genetic polymorphism of UGT could be a major factor responsible for the observed inter-individual differences (Iyer, 1999). However, the molecular mechanisms of these variations have been poorly elucidated. To date, few variant UGT proteins have been described (Ciotti et al., 1997;Lévesque et al., 1997;Coffman et al., 1998;Lévesque et al., 1999). Identification and characterization of additional polymorphisms are essential in order to address the exact role of UGT genetic variations in individual response to therapeutic drugs in addition to their role in disease susceptibility. The present study was designed to investigate the extent of polymorphic variations in one member of the UGT1A family, the *UGT1A7* gene, using a combination of polymerase chain reaction (PCR) single-strand conformation polymorphism (SSCP) and sequencing analysis of germline DNA from Caucasian and African-American individuals. The UGT1A7 isoenzyme is a typical example of an extrahepatic UGT, with undetectable expression of the UGT1A7 transcript in human liver (Strassburg et al., 1997b). Among substrates efficiently conjugated by UGT1A7 are several phenolic compounds, carcinogens, flavonoids, anthraquinones and drugs as determined using an in-vitro system (Strassburg et al., 1998;Ciotti et al., 1999). We report the presence of six single nucleotide polymorphisms in the coding region of UGT1A7, all identified in the substrate binding domain. Population studies revealed the existence of four distinct *UGT1A7* alleles present in both Caucasian and African-American populations. In addition, we conducted functional studies to evaluate the impact of these genetic alterations on the catalytic activities of the UGT1A7 variant proteins towards specific substrates, and looked at the expression pattern of this UGT1A isoenzyme in human tissues.

In the present work, we identify and report the characterization of functional polymorphisms in the *UGT1A7* gene. The results presented suggest that a low UGT1A7 conjugator genotype is present in a large proportion of the Caucasian population and results in a reduced velocity of the enzyme. The present findings raise the possibility that these inherited variations in the *UGT1A7* gene may have a considerable impact on the efficient glucuronidation of specific substrates, including human carcinogens and drugs.

Materials and methods

Subjects

Genomic DNA obtained from blood donors, was isolated from immortalized lymphocyte cell lines (n = 144) obtained from the Massachusetts General Hospital. The samples were collected from normal healthy blood donors in the Boston area. Details on the study population were published previously (Bell et al., 1999).

Polymorphism detection

Total genomic DNA from immortalized lymphocyte cell lines and human cancer cell lines derived from 36 unrelated individuals were used as the template to amplify PCR products for SSCP analysis. Three primer pairs were designed to amplify the UGT1A7 exon 1 coding region from nucleotides –36 to 1013 (Genbank accession number HSU39570) in three overlapping fragments: 120 and 121 (nucleotides –36–306), 122–123 (nucleotides 290–588) and 124–126 (nucleotides 570–1013) (Table 1). The specificity of the primers was verified by automated sequencing of the PCR products. The PCR was performed for all three sets of primers in the presence of radiolabelled forward primer in a volume of 25 µl using the hot-start technique (Chou et al., 1992) and the following conditions: five cycles of 30 s at 94 °C, 45 s at 60 °C and 60 s at 72 °C, followed by 30 cycles of 30 s at 94 °C, 45 s at 55 °C, and 60 s at 72 °C. An initial denaturation at 94 °C for 5 min and a final extension at 72 °C for 10 min were used. PCR products were mixed with two volumes of stop solution (95% deionized formamide, 10 mM NaOH, 0.05% each of bromophenol blue and xylene cyanol dyes), denatured at 94 °C for 2 min, cooled on ice and loaded into a 0.5 × Hydrolink-MDE gel (AT Biochem, Malvern, PA, USA). Electrophoresis was performed at 30 W in the cold room for 4 h in 0.6 × TBE. After drying on Whatman paper, the gel was exposed to film at room temperature for 24 h.

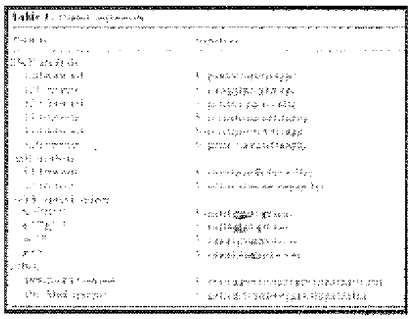


Table 1. Primer sequences

[Help with image viewing]

[Email Jumpstart To Image]

Direct sequencing and confirmation of polymorphism

To ensure specific amplification of UGT1A7, PCR products from all sets of primers were purified using Qiagen quick columns (Qiagen Inc., Santa Clarita, CA, USA) for the removal of PCR primers, and sequenced by the ABI 377 automated sequencer. The same procedure was used for aberrant conformers observed in the SSCP analysis to identify UGT1A7 variants, prior to sequencing analysis.

Genotyping

To genotype the study population, new PCR primers (#51 and #52, Table 1) were designed to specifically amplify the UGT1A7 first exon (bases −76 to 1048 in Genbank HSU39570), which would include all the newly discovered polymorphisms. For hybridization analysis of the UGT1A7 amplification products, allelic specific oligonucleotides (ASOs) were designed to detect missense mutations. Each ASO represents a 17-mer centered on the polymorphic nucleotide of each variant. Sequences of the PCR primers and the ASOs are presented in Table 1. PCR amplifications were performed on 20 ng of genomic DNA in 50 µl aliquots containing 20 pmol of each primer, 1 × reaction buffer (50 mM KCl, 1.5 mM $MgCl_2$, and 10 mM Tris pH 8.5), 100 µM dNTPs, 4% DMSO, and 2 U of *Taq* DNA polymerase (PE Applied Biosystems, Branchburg, NJ, USA). The amplification conditions were: denaturation at 94 °C for 5 min, five cycles of 60 s at 94 °C, 45 s at 62 °C and 90 s at 72 °C, followed by 30 cycles of 60 s at 94 °C, 45 s at 56 °C, and 90 s at 72 °C, with a final 7 min extension at 72 °C. Aliquots of the PCR products (20 µl) were denatured by alkali treatment using 200 µl of a solution of 0.5 M NaOH, 2.0 M NaCl and 25 mM ethylenediaminetetraacetic acid (EDTA). An aliquot (50 µl) of each PCR product was spotted onto four Hybond N^+ filters (Amersham, Arlington Heights, IL, USA) using a 96-dot blot apparatus. Filters were prehybridized for 2 h in tetramethylammonium chloride (TMAC) buffer containing 3.0 m TMAC, 0.6% SDS, 1 mM EDTA, 10 mM Na_3PO_4 (pH 6.8), 5 × Denhardt's, and 40 µg/ml yeast RNA. All filters were then hybridized overnight at 52 °C in 10 ml TMAC buffer in the presence of 10 pmol ^{32}P-labelled ASOs and a 50-fold excess of cold-competitor oligo of the opposite allele. All blots were washed for 20 min at room temperature in TMAC Wash Buffer (3 M TMAC, 0.6% SDS, 1 mM EDTA, and 10 mM Na_3PO_4 pH 6.8) followed by 20 min at 54 °C. Filters were exposed on film at room temperature for 24 h.

Stable expression of human UGT1A7 alleles

Full length cDNA encoding UGT1A7 was isolated from a human renal adenocarcinoma cell line (786–0). The presence of the UGT1A7 transcript was demonstrated in this cell line by RT-PCR in the present study. Total RNA (5 µg), collected from the cells with Trizol (Gibco BRL, Grand Island, NY, USA) following the manufacturer's instructions, was used to synthesize cDNA. Oligo(dT)-primed cDNA was synthesized using a SuperScript II cDNA synthesis kit (Gibco BRL) according to the manufacturer's specifications. An aliquot of the first-strand cDNA was used as the template for PCR amplification of UGT1A7 using reading proof DNA polymerase, Turbo *Pfu* DNA polymerase (Stratagene, La Jolla, CA, USA). Two primers were used to introduce restriction endonuclease cleavage sites upstream of the Kosak translation initiation sequence at the 5' end, and at the 3' end in frame with the *C*-terminal tag encoding the *myc* epitope and a polyhistidine metal-bonding peptide of the mammalian expression vector, pcDNA3.1/Myc-His (Invitrogen, San Diego, CA, USA). The PCR product was digested with *Eco* RI/ *Xho* I and directionally cloned into the pcDNA3.1/Myc-His vector to generate pcDNA3.1/Myc-His –*UGT1A7*3*. The sequence of the insert was verified by automated sequence analysis on an ABI 377 using specific UGT1A7 primers. The expression of the recombinant gene was tested by in-vitro transcription/translation analysis and confirmed by Western analysis using anti-*myc* antibody to detect UGT1A7 protein (Invitrogen) (data not shown).

Expression vectors encoding the three other UGT1A7 variants were prepared using a Quickchange PCR site-directed mutagenesis kit (Stratagene) and pcDNA3.1/Myc-His -UGT1A7*3 as the starting plasmid. After generating **2* and **4* from

**3*, **1* was generated using **4* as template. Duplicate PCR reactions (50 µl total volume) contained 0.5 ng/µl template plasmid, 0.25 µM forward primer and reverse primer, 1 ×*Pfu* reaction buffer (10 mM KCl, 10 mM $(NH_4)_2SO_4$, 20 mM Tris-HCl, pH 8.8, 2 mm $MgSO_4$, 0.1% Triton X-100, 0.1 mg/ml nuclease-free bovine serum albumin), 0.2 mM Quickchange dNTP mixture, and 2.5 U of the high fidelity *Pfu* Turbo polymerase. The forward and reverse primers for changing R^{208} to W^{208} were 5'-CAAGGAGAGAG TACGGAACCACATCATGCAC-3' and 5'-GTGCATGA TGTGGTTCCGTACTCTCTCCTTG-3' and for changing K^{129} K^{131} to N^{129} R^{131} were 5'-CAAGGAGAG AGTATGGAACCACATCATGCAC-3' and 5'-GTGCAT GATGTGGTTCCATACTCTCTCCTTG-3', respectively. Following PCR, the reaction contents were diluted 1:1 with 1 ×*Pfu* reaction buffer and digested with *Dpn* I (10 U) for 30 min at 37 °C prior to transformation of *Escherichia coli* XL1-Blue (Stratagene). An expression vector carrying the desired mutation(s) was obtained from each duplicate PCR reaction generating the plasmids, pcDNA3.1/Myc-His –*UGT1A7* *1–*34a* and **1–35a*, **2–32a* and **2–33a*, and **4–1a* and **4–2a*.

To prepare HEK cell populations stably transfected with each of the pcDNA3.1-Myc-His-UGT1A7 expression plasmid, cell culture dishes were seeded with 3.5×10^6 exponential-phase HEK cells maintained in Dulbecco's-modified Eagle's medium (DMEM) containing 10% fetal calf serum (complete medium). The next morning the cells were washed with serum-free DMEM and overlaid with 3 ml DMEM containing 25 µg of Lipofectin (Gibco BRL) and 20 µg of the appropriate pcDNA3.1-Myc-His-UGT1A7 expression plasmid. The transfections were stopped after 6 h by addition of fresh DMEM with 10% fetal calf serum, and following an additional 48 h culture period, G418 (1 mg/ml) was added to begin the process of selecting pcDNA3.1-Myc-His-UGT1A7-expressing cell populations. During the next 2 weeks, fresh G418-containing medium was added every 3 days until colonies of resistant cells became visible. Thereafter, the concentration of G418 in the culture medium was reduced to 0.5 mg/ml to allow for outgrowth of the G418-resistant cell populations.

For the analysis of UGT1A7 expression and enzyme activities, membrane fractions were prepared from 800×10^6 cells of each population. Cells were harvested using trypsin-EDTA treatment to release the cell monolayer, collected in centrifuge tubes, centrifuged at 500 ***g***, and resuspended in ice-cold phosphate-buffered saline (PBS). After repeating the wash step, the cell pellets were resuspended in 0.25 M sucrose, homogenized using a glass homogenizer, and centrifuged for 20 min at 5000 ***g*** to remove nuclei and other particulates. The membrane fractions were then collected by sedimentation at 100 000 ***g*** for 1 h followed by resuspension of the membrane pellet in buffer containing 0.1 M potassium phosphate, pH 7.5, 1 mM EDTA, and 20% glycerol. Protein concentrations were determined by the bicinchononic acid method (Smith et al., 1985) using 0.5% SDS as the assay diluent.

Immunoblot blot analysis of UGT1A7

Relative UGT1A7 expression levels in the stable UGT1A7-expressing cell populations were determined by a semiquantitative immunoblot analysis method essentially as described previously (Ritter et al., 1999) but substituting polyclonal antisera raised against human UGT1A9 amino terminal residues 31–191. Briefly, membrane proteins were resolved by electrophoresis through SDS–7.5% polyacrylamide gels and electroblotted onto nitrocellulose membranes. After the blocking step, blots were incubated for 1 h at room temperature in UGT1A9 antisera diluted 1 : 1000 in TBS-T (Tris-buffered saline with 0.2% Tween 20) containing 5% dry milk. Blots were washed and then incubated overnight in solution containing the secondary antibody (horseradish peroxidase-conjugated rabbit antimouse IgG, Amersham) diluted 1 : 20 000 in TBS-T containing 5% blocking reagent. The next morning, blots were washed extensively for 2 h at RT with several changes of TBS-T prior to detection of horseradish peroxidase using an enhanced chemiluminescence ECL kit and Kodak XB-1 film (Amersham). Digitalized film images were recorded using a Fotodyne video camera system and analysed using Scion Image for Windows, a PC version of NIH Image (Scion Corporation, Frederick, MD, USA). Linearity in the detection signal was demonstrated by parallel analysis of serially diluted *UGT1A7* *3. Levels of proteins were confirmed using a monoclonal c-myc antibody, and similar results were obtained (data not shown).

Functional UGT enzyme assays

UGT activities towards 3-OH-, 7-OH-, 8-OH-, and 9-OH-B(a)P and B(a)P-*trans*-(–)-7,8-dihydrodiol were determined as previously described (Grove et al., 1997) with slight modifications. Reactions (50 µl volume) contained 100 mM potassium phosphate, pH 7.5, 6 mM $MgCl_2$, 6 mM d-saccharo-1,4-lactone, 1.5 mM UDP-glucuronic acid, 0.2 µCi [^{14}C]-UDP-glucuronic acid (Dupont-NEN), 2 mg/ml membrane protein, and benzo(a)pyrene (B(a)P) phenol substrate (16.6–300 µM) (Chemsyn, Kansas City, MO, USA) added in 2 µl dimethylsulfoxide. Under the conditions of the assay, formation of B(a)P 7-O-glucuronide from 7-OH-B(a)P was found to be proportional to both time and protein concentration. Due to the lack of apparent enzyme latency, inclusion of detergent was found to be unnecessary for assessment of the full glucuronidating potential of UGT1A7-expressing HEK cell membranes.

Expression analysis of UGT1A7

Tissue samples and cell lines were obtained from Clontech Laboratories Inc. (Palo Alto, CA, USA) and the American Type Tissue Collection (ATCC, Rockville, MD, USA), respectively. Total RNA was collected with Trizol (Gibco BRL) and UGT1A (5'-GTATGTGTATTTGCCACAATTG-3') and GAPDH (5'-TGGGTGTGAACCATGAG-3') specific primers were used to synthesize cDNA from total RNA (5 µg) using a SuperScript II cDNA synthesis kit (Gibco BRL) according to the manufacturer's specifications. Aliquots of the first-strand cDNA were used as templates for PCR amplification of UGT1A7 and GAPDH transcripts using *Taq* DNA polymerase (PE Applied Biosystems). PCR was carried out using the forward primer, 5'-TGCCGATGCTCGCTGGACG-3' and the reverse primer, 5'-CCAATGAAGACCATGTT GGGC-3' for UGT1A7 and gave a product of 539 bp (Strassburg et al., 1997a); the forward primer, 5'-TGGGTGTGAACCATGAG-3' and the reverse primer, 5'-CCCAGCGTCAAAGGTGG-3' were used for the amplification of GAPDH, in the following conditions: 94 °C for 5 min following by 30 cycles of 94 °C for 1 min, 64 °C for 1 min, 72 °C for 1 min 30 s, and a final extension time of 10 min at 72 °C. With all RT-PCR reactions, a parallel aliquot of the same sample was run in which reverse transcriptase was omitted. The RT-PCR amplification products were analysed by agarose gel electrophoresis and by direct sequencing with an ABI automated sequencer to confirm the identity of UGT1A7.

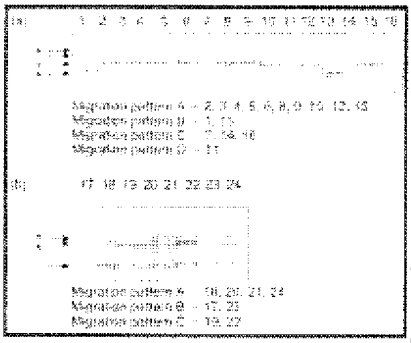
Statistical analysis

Differences between UGT1A7 variant groups were analysed by ANOVA (analysis of variance). When significant differences between groups existed, the groups were further compared using a Bonferroni post-test. Differences between groups were considered statistically significant when $P <= 0.005$.

Results

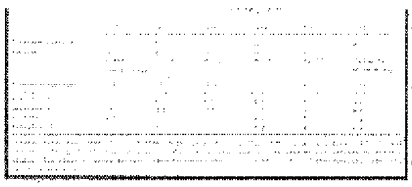
Identification of three missense mutations in the human UGT1A7 gene

To determine if UGT1A7 was genetically polymorphic, the entire sequence of the UGT1A7 exon 1 was analysed, including the intron boundaries. We examined the UGT1A7 genomic sequence of 36 unrelated individuals using a combination of PCR-SSCP and sequence analysis. Twenty-eight of the 36 individuals used in the polymorphism screening were Caucasian individuals whereas the remaining eight germline DNA samples were of African ancestry. Three sets of primers (120–121, 122–123 and 124–126) were designed to specifically amplify the genomic region encoding UGT1A7 (Table 1). Following SSCP analysis, several migration patterns were identified with all three sets of primers. One detectable difference in the migration was observed using primers 120 and 121 which amplified the 5' portion of the first exon of UGT1A7. Four migration patterns were identified using primer set 122–123 (middle part of the exon 1 of UGT1A7) and three in the case of primer set 124–126 (3' end of the exon 1 of UGT1A7) (Fig. 1). All differential aberrant migrations were attributed to specific sequence variations including silent changes and missense mutations, as confirmed by automated sequence analysis using the ABI377 as summarized in Table 2.



[Help with image viewing]
[Email Jumpstart To Image]

Fig. 1. Identification of UGT1A7 polymorphisms using PCR-SSCP analysis. SSCP analysis of the exon 1 of *UGT1A7* gene including flanking intron boundaries. Three sets of primers which specifically amplified UGT1A7 were used. Sequences of all primers are listed in Table 1. (a) Showing PCR products amplified using primers 122–123 and (b) PCR products amplified using primers 124–126. SSCP analysis of PCR products amplified using primers 120 and 121 is not shown. All amplicons were analysed on MDE gel as described in Materials and Methods. Arrowheads indicate the presence of a band and stars point out the band which varies from one sample to another and indicates the presence of potential polymorphisms. Samples were grouped according to specific migration patterns, characterized by the number of bands and their position. Four migration patterns were identified using primers 122–123 (a), whereas three were observed in the case of PCR products obtained using primers 124–126 (b).

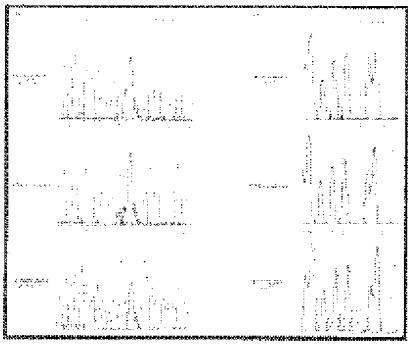


[Help with image viewing]
[Email Jumpstart To Image]

Table 2. Polymorphic genetic variations identified in the *UGT1A7* gene [a]Relative to the start codon ATG. [b]Only observed in African-American. [c]Nucleotide changes at positions 387, 391 and 392 are in linkage. [d]Genbank accession number HSU 39570. [e]Determined by ASO analysis and confirmed by sequence analysis. [f]Individuals of African ancestry. [g]Allele frequency codon 11 (c =0.89;a =0.11). [h]Allele frequency codon 252 (g =0.71;a =0.29).

Sequence analysis of the aberrant shift in the migration pattern of the PCR product amplified using primers 120–121, revealed the presence of one nucleotide change (C to A transversion), corresponding to a silent change at codon 11. This silent change was observed only in individuals of African-American ancestry. The genotyping data obtained by ASO analysis determined in 30 unrelated individuals of African ancestry, showed a frequency of 0.11 for the variant allele (A^{11}) and 0.89 for the previously reported allele (C^{11}).

Sequencing of all PCR products showing aberrant migration on the SSCP analysis revealed three nucleotide changes in the PCR fragment obtained with primers 122–123, which amplifies the middle part of the 1A7 first exon. Within six base pairs, three nucleotides were changed revealing a T^{387} to G transversion, a C^{391} to A transversion, and a G^{392} to A transition. The band shift observed using the primer set 124–126 was explained by one missense mutation caused by a T^{622} to C transition. An additional band shift was explained by the presence of one single-nucleotide substitution leading to a silent change at position 756 (Table 2). Figure 2 illustrates the sequence analysis of homozygous and heterozygous individuals for all missense mutations discovered in the present study.



[Help with image viewing]
[Email Jumpstart To Image]

Fig. 2. Confirmation of the presence of polymorphic variations in the *UGT1A7* gene by automated sequence analysis. Sequence analysis of PCR products amplified from individuals showing aberrant shift in the SSCP analysis. Only the functional polymorphisms at codon 129, 131 (a) and 208 (b) are illustrated. Silent changes also confirmed by sequence were observed in the PCR product 120–121 and 122–123. All three genotypes at both loci are illustrated.

Presence of four distinct UGT1A7 alleles and their distribution in the population

The three missense mutations were observed in different combinations resulting in the existence of four *UGT1A7* alleles. The previously described *UGT1A7* allele corresponds to the *UGT1A7*1* ($N^{129}R^{131}W^{208}$) allele (Genbank HSU39570 and HSU89507). The alleles *UGT1A7*2*, **3* and **4* correspond to $K^{129}K^{131}W^{208}$ (Genbank AF110191), $K^{129}K^{131}R^{208}$ (Genbank AF110192) and $N^{129}R^{131}R^{208}$ (Genbank AF110193), respectively (Table 3).

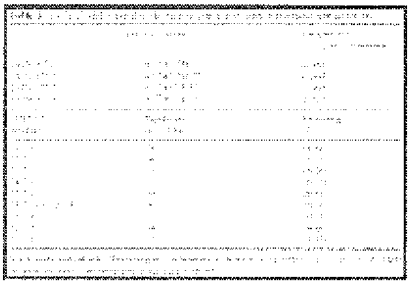


Table 3. UGT1A7 alleles found in the human population: allele frequencies and genotypes [a]Caucasian individuals. [b]Heterozygous individuals at both loci are either **1/*3* or **2/*4*. Allele frequencies were calculated assuming they were all **1/*3*.

[Help with image viewing]
[Email Jumpstart To Image]

Haplotype analysis of two CEPH families and additional unrelated individuals revealed that the polymorphisms at positions 129 and 131 are in linkage, whereas the polymorphism at position 208 occurs independently, confirming the presence of four alleles in the human population (Table 2 and Fig. 3). In the first family studied (Fig. 3a), the genotyping data show that individual #11 is homozygous for N/R at positions 129/131 and R at position 208, whereas individual #12 is homozygous for K/K at positions 129/131 and W at position 208. In the second family (Fig. 3b), the observation that one of the children (#3) carried two *UGT1A7 *1* alleles demonstrates that both parents (individuals #1 and #2), heterozygous for both missense mutations (**1/*3* or **2/*4*), are in fact heterozygous *UGT1A7*1* and **3*. This result shows that in this case, all missense mutations are present on the same chromosome. In addition, haplotype analysis of additional unrelated individuals revealed that the two single nucleotide substitutions at position 622 and 756 are not in linkage (Table 2).

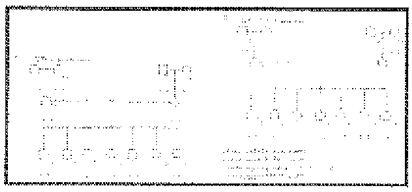
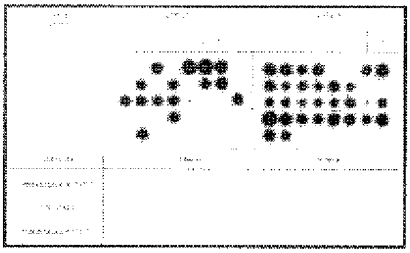


Fig. 3. Genotyping analysis of two CEPH families. Haplotype analysis of three missense mutations present in the *UGT1A7* gene. Genotyping was performed by ASO hybridization method and confirmed by sequencing. Haplotypes at positions 129, 131 and 208 are shown for each member of a family from Utah (a) and a French family (b).

[Help with image viewing]
[Email Jumpstart To Image]

We subsequently examined the distribution of the UGT1A7 single nucleotide polymorphisms (SNPs) among Caucasian samples. To determine the frequency of each four alleles, we genotyped a control population of 144 unrelated Caucasian individuals using the ASO hybridization method. This technique allows simultaneous genotyping of a large number of arrayed samples in DNA dot blot format at low cost and high efficiency. Briefly, the first exon of UGT1A7 was amplified using primers 51 and 52, as described in Materials and Methods. After denaturation, the PCR products were spotted onto four filters, each subsequently hybridized with a single ASO (sequence in Table 1). Four ASOs were designed to hybridize specifically to the sequence corresponding to NR or KK at position 129 and 131, and W or R at position 208. As illustrated in Fig. 4 for the genotyping at position 129 and 131, a positive signal observed only with the labelled ASO $N^{129}R^{131}$ indicates the individual is a $N^{129}R^{131}$ homozygote, a positive signal using both ASOs indicates the individual is a heterozygote, whereas a positive signal detected only using the labelled ASO $K^{129}K^{131}$ identifies the individual as homozygous $K^{129}K^{131}$. The two remaining filters were used to determine the genotype at position 208 and were hybridized with ASOs W^{208} and R^{208} (data not shown).



[Help with image viewing]
[Email Jumpstart To Image]

Fig. 4. Allelic-specific oligonucleotide hybridization. For the genotyping at all polymorphic sites (129, 131 and 208), a single PCR product was amplified from germline DNAs from unrelated individuals using primer sets 51 and 52 (see Table 1 for sequence). PCR products were denatured and spotted onto four Hybond N+ filters. Each filter was hybridized separately with specific ASOs designed to detect polymorphism variations at all 3 positions. In addition, a 50-fold excess of cold competitor oligo of the corresponding opposite allele was added during the hybridization to improve the signal to noise ratio. Filters were washed as described in the Materials and Methods section and exposed on film for 16–24 h at room temperature.

Genotyping results showed that only 14.6% of this population was homozygous for the previously described *UGT1A7 *1* allele ($N^{129}R^{131}W^{208}$) (Table 3). Homozygosity for *UGT1A7 *2* and *UGT1A7 *3* was observed at frequencies of 6.3% and 15.3% in this population. In contrast, the allele *UGT1A7 *4* was found to be rare, with 0.7% of the population homozygous for **4/*4*. In the case of individuals who were heterozygous at both loci, two genotypes were possible, **1/*3* or **2/*4*. The haplotype in these individuals was not determined for all samples. Since the frequency of *UGT1A7 *4* allele is very low, it may be assumed that most of these individuals (n = 30 individuals, 20.80%) represent **1/*3* heterozygotes. In addition, direct determination of haplotype using a carbon nanotube-based DNA sequence determination using atomic force microscopy showed that the few samples analysed were heterozygous **1/*3* (Woolley et al., in press).

The *UGT1A7 *1* allele and the *UGT1A7 *3* allele (containing all three missense mutations) showed similar frequencies in the Caucasian population, 0.358 and 0.361, respectively. While, the alleles *UGT1A7 *2* and *UGT1A7 *4* presented lower frequencies of 0.264 and 0.017, respectively. All four alleles were observed in the small African-American population studied (data not presented). The allele frequencies and genotype analysis were not determined due to the small number of samples available.

Function of the UGT1A7 protein is affected by the newly found polymorphisms

To characterize the glucuronidating activities of the four *UGT1A7* allelic variants, pcDNA3.1-Myc-His-based expression vectors encoding each of the variants were prepared and transfected into HEK cells for selection of G418-resistant permanent transfectants. The relative level of expressed UGT1A7 protein in membrane fractions prepared from each cell population was determined by immunoblotting with a polyclonal human UGT1A9 antibody directed against amino terminal residues 31–191 (Fig. 5), and was confirmed using a monoclonal c-myc antibody (data not shown). Consistent with the high amino acid identity of the UGT1A7 and UGT1A9 amino termini (78% identity), crossreactivity of the 1A9 antibody was observed towards human UGT1A7. The major immunoreactive band detected in the UGT1A7-expressing HEK cell membranes (Fig. 5) had slightly reduced mobility compared to the intense UGT1A9 band of human liver microsomes, and it was not observed in the control (untransfected) cell membranes. The level of expression of UGT1A7 protein was found to vary among the four populations, from a low of 0.16 relative units in the *UGT1A7*1*-expressing cell population to a high of 1.0 in the *UGT1A7*3*-expressing cells. This difference in relative level of expression was reproducible in different batches of transfected cells and appeared to be a function of the level of glucuronidating activity specified by each allele (described in more detail below).

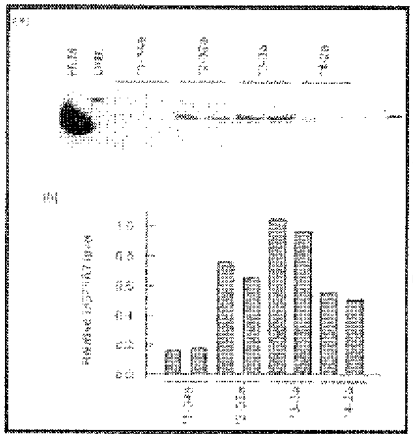
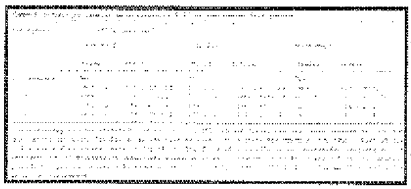


Fig. 5. Relative expression of the UGT1A7 alleles. Membrane fractions prepared from HEK cells expressing the four different UGT1A7 variants (30 μg protein loaded in each lane) were subjected to SDS-polyacrylamide gel electrophoresis followed by electrotransfer onto nitrocellulose and immunoblot analysis with antisera raised against human $UGT1A9_{31--191}$. (a) Enhanced chemiluminescence (ECL) image. HLM, human liver microsomes. Untr., untransfected control HEK cells. (b) Relative levels of UGT1A7 determined by semiquantitative densitometric analysis of the ECL image.

[Help with image viewing]
[Email Jumpstart To Image]

For comparison of the glucuronidating activities of the variants, we selected several B(a)P metabolites as substrates, including the 7-OH and 8-OH phenolic derivatives which were reported previously as human UGT1A7 substrates (Strassburg et al., 1998). The data for 3-OH, 7-OH, and 9-OH-B(a)P are presented in Table 4. No glucuronidating activity towards any of these three substrates could be detected in membranes prepared from the untransfected control cells. In contrast, membranes from each of the four UGT1A7 variant-expressing cell populations catalysed the glucuronidation of the 7-phenol at the highest rate followed by the 3- and 9-phenols. Activity towards the 8-phenol was also detected, but the analysis of this activity was complicated by its labile nature. In contrast to the phenols, no activity could be detected towards B(a)P-7,8-dihydrodiol, reflecting a strong preference of the enzyme for planar hydroxyl groups.



[Help with image viewing]
[Email Jumpstart To Image]

Table 4. Relative glucuronidating activities of UGT1A7 variants towards B(a)P phenols
Glucuronidating activities of UGT1A7 variant-expressing HEK cell membranes were determined towards the indicated B(a)P phenol substrates. The data shown represent the mean ± SD of three determinations. The relative B(a)P phenol UGT activities of the variants were calculated by dividing the absolute activities by the corresponding fractional level of expressed UGT1A7 determined by immunoblot analysis (0.16 for **1*, 0.64 for **2*, 1.0 for **3*, and 0.48 for **4*). Values in parentheses represent the ratio of the mean to that of the **3* cell population. [a] $P <= 0.01$ *vs.* **2* group. [b] $P <= 0.02$ *vs.* **3* group. ND, not detected.

As shown in Table 4, the absolute glucuronidating activities of the four variants towards any of the active substrates varied by only approximately two-fold, with the membranes from the **2* expressing cell population having the highest activity followed by **3*, **4* and **1* in that order. Upon taking into account the differences in relative UGT1A7 expression level, it was apparent, however, that the **1* form had the highest relative activity followed by **2*, **4* and **3*. The same relative order of activity applied to each substrate. The difference between **1* and **2* ($P <= 0.01$ level) indicates that $N^{129}R^{131}$ is advantageous compared to $K^{129}K^{131}$ for high glucuronidating activity. Similarly, the difference between **2* and **3* ($P <= 0.02$) indicates that substitution of W for R at position 208 enables higher catalytic activity.

To determine if these observed differences were due to alterations in apparent K_m or V_{max}, a kinetic analysis was carried out using 7-OH-B(a)P as a probe substrate. A representative Lineweaver–Burk plot for 7-OH-B(a)P is shown in Fig. 6. The apparent different *y*-intercepts (equal to $1/V_{max}$) and common *x*-intercept (equal to −1/apparent K_m) of the four plots (determined by linear regression analysis) suggests that the enzymes differ in V_{max} rather than apparent K_m. Although the group means for relative V_{max} determined in three independent experiments were found not to differ statistically using the Bonferroni method for multiple group comparison, the **1* population exhibited an average 5.8-fold higher relative V_{max} compared to **3*, and a 2.6- and 2.8-fold higher relative V_{max} than **2* and **4*, respectively (Table 5).

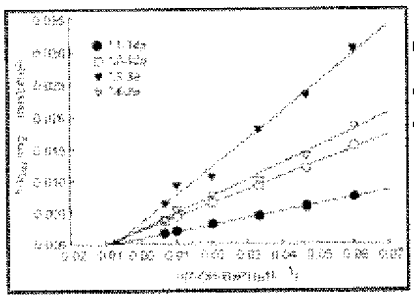
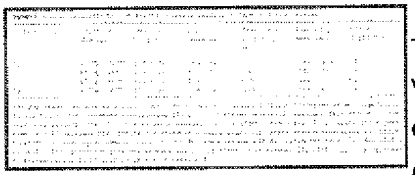


Fig. 6. Lineweaver–Burk plot of 7-OH-B(a)P UGT activities catalysed by UGT1A7 allelic variants. The effect of altering the 7-OH-B(a)P concentration on the rate of 7-OH-B(a)P glucuronidation by membranes from HEK cells expressing the four different UGT1A7 variants is presented as a Lineweaver–Burk plot. V *Rel* represents the absolute 7-OH-B(a)P glucuronidation rate (pmol/mg/min) divided by the relative level of expressed UGT1A7 variant.

[Help with image viewing]
[Email Jumpstart To Image]



[Help with image viewing]
[Email Jumpstart To Image]

Table 5. Kinetic parameters for 7-OH-B(a)P UGT activity catalysed by human UGT1A7 variants The data shown represent the average ± SD for the K_m and V_{max} values determined in three independent experiments. K_m and V_{max} in each experiment were determined from linear regression analyses of Lineweaver–Burk plots of 1/[7-OH-B(a)P concentration] versus 1/7-OH-B(a)P glucuronidation rate. The relative level of UGT1A7 in membranes prepared from UGT1A7-expressing HEK cells was determined by semiquantitative immunoblot analysis using antisera to human $UGT1A9_{31-191}$ assigning an arbitrary value of 1.0 to the clonal cell line with the highest expression (*3). The relative levels of UGT1A7 proteins were further confirmed using a monoclonal c-myc antibody. The relative V_{max} was calculated by dividing the V_{max} by the relative level of expressed UGT1A7.

Expression analysis of UGT1A7

We ascertained the expression of the UGT1A7 transcript by RT-PCR analysis of human liver, human lung and cell lines derived from metabolizing tissues including liver (HepG2), colon (Colo-320) and kidney (786–0). Liver tissue and the hepatocarcinoma cell line, HepG2 showed no amplification of the UGT1A7 PCR product. In contrast, the presence of a single RT-PCR product corresponding to UGT1A7 was observed in human lung (Fig. 7). Specific amplification of UGT1A7 was also detected in cell lines derived from colon and kidney. In contrast, the normalizing control mRNA, GAPDH, was amplified to a similar extent in all of the cell lines tested and the human liver and lung samples.

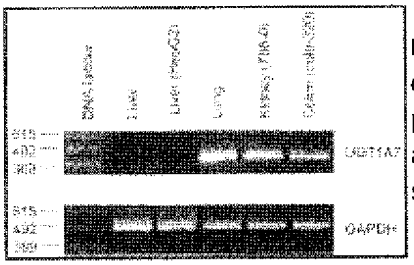


Fig. 7. Tissue-specific expression of UGT1A7. The presence of UGT1A7 transcript was determined by RT-PCR analysis using specific primers (18). The RT-PCR amplification products (UGT1A7 and GAPDH, top and bottom panel, respectively) were analysed by agarose gel electrophoresis. Identity of UGT1A7 was further confirmed by direct sequencing of the RT-PCR products.

[Help with image viewing]
[Email Jumpstart To Image]

Discussion

The present study aimed to identify novel common polymorphisms in the human *UGT1A7* gene in the general population. We restrained our search of polymorphic variations to the first exon of *UGT1A7* (intron–exon boundaries

included) which codes for the proposed substrate-binding domain. Although a relatively small number of unrelated individuals were screened for the presence of constitutive genetic alterations, this approach allowed us to identify six SNPs in the 1050-bp region scanned. This locus was found to be highly polymorphic with one polymorphism found every 175 bp within the coding region. The frequency of SNPs found in the coding region of the *UGT1A7* gene is very similar to what has been reported in other metabolizing enzyme genes such as cytochrome P450 (Cargill et al., 1999;Halushka et al., 1999). All six newly identified SNPs in UGT1A7 were found in the coding region. Three were missense mutations in codons 129, 131 and 208, characterized by the substitution of N to K, R to K and W to R, respectively. A haplotyping study with two CEPH families revealed that the nucleotide substitutions at codons 129 and 131 were in linkage, whereas the third mutation at codon 208 was unlinked.

The identification of variant forms of UGT proteins in the human population is a crucial step in elucidating the functional importance of UGT genetic polymorphisms. These studies should lead to a better understanding of the role of inter-individual variability in the glucuronidation pathway on disease susceptibility and clinical drug responses. In the *UGT1* gene complex (estimated to be more than 500 kbp in length), only approximately 30 alleles have been identified to date (Mackenzie et al., 1997), and most of these have been associated with the *UGT1A1* (bilirubin UDP-glucuronosyltransferase) gene. Among these, four common allelic variations in the TATA box of the UGT1A1 promoter have been shown to influence expression of UGT1A1 and associate with the hyperbilirubinemia characteristic of Gilbert's disease (Bosma et al., 1995;Monaghan et al., 1996;Beutler et al., 1998;Guillemette et al., 2000). Additional constitutive variation in the *UGT1A6* gene has also been observed, where two close missense mutations in the substrate binding domain were shown to alter the catalytic activities for specific therapeutic agents (Ciotti et al., 1997). The present study constitutes the first report of the presence of genetic polymorphisms in the *UGT1A7* gene. Population studies revealed that the four distinct *UGT1A7* alleles are not restricted to the Caucasian population but were also observed in the African-American population.

The new form of UGT1A7 protein, corresponding to the allele *UGT1A7*3* ($K^{129}K^{131}R^{208}$), differs from the previously described UGT1A7 protein by three amino acids, as a result of the three missense mutations. Although the substitution of arginine to a lysine at position 131 appears as a conservative change, the linked substitution of an asparagine at position 129 to a lysine results in the change of an uncharged polar amino acid to a positively charged amino acid. The conversion of the apolar tryptophan to a positively charged, hydrophilic arginine at position 208 also appears non-conservative. Each change has the potential to alter the structure and function of UGT1A7, if they occur in a critical domain of the enzyme. Our analysis using B(a)P metabolites as model substrates for UGT1A7 (Strassburg et al., 1998) suggested that each difference can independently affect the UGT1A7 catalytic activity, and that their effects are additive. The previously described wild-type form, *UGT1A7*1*, exhibited the highest relative activity, whereas *UGT1A7*3*, which possesses variant amino acids at both positions (129/131 and 208) had the lowest. Furthermore, it appeared that the relative catalytic activities of the four variants were independent of the substrate, with 3-OH- and 9-OH-B(a)P yielding results similar to 7-OH-B(a)P. Although further studies are necessary, these data suggest that other UGT1A7 substrates might also be affected. These are known to include phenols (4-nitrophenol, 2-hydroxybiphenyl, propyl- and octyl-gallate and vanillin), naphthols, anthraquinones, coumarins, and certain steroid hormone derivatives (estriol, 2-hydroxyestradiol, and 4-hydroxyestrone) (Strassburg et al., 1998). The impact of the UGT1A7 polymorphisms on the glucuronidation of these compounds *in vivo* will depend on many factors, including the relative contribution of the UGT1A7 isozyme to the total glucuronidation of each substrate.

The location of the amino acid substitutions in the proposed substrate-binding domain of the enzyme suggested that the alteration in catalytic activity may be due to altered substrate-binding affinity (K_m). However, kinetic analysis using 7-OH-B(a)P as substrate failed to provide convincing evidence of an effect on enzyme K_m. In contrast, greater effects were observed on enzyme V_{max}, where the UGT1A7 form presenting all three missense mutations (*UGT1A7*3*) had a 5.8-fold lower relative V_{max} value compared to the *UGT1A7*1* wild-type. This finding is consistent with two other reports that amino acid variation in the putative UGT substrate-binding domain, at positions 181/184 of UGT1A6 (Ciotti et al., 1997) and position 85 of UGT2B15 (Lévesque et al., 1997), affects enzyme V_{max} and not K_m.

As illustrated in Fig. 8, both regions of the protein that present the new missense mutations are highly conserved in UGT1A7 of lower species, and among closely related UGT1A family members, namely UGT1A8, 1A9 and 1A10. With respect to the specific amino acid identities at positions 129/131 and 208, human UGT1A8 ($K^{129}K^{131}W^{208}$), UGT1A9 ($K^{129}K^{131}R^{208}$), and UGT1A10 ($N^{129}R^{131}W^{208}$) resemble the *UGT1A7*2*, **4*, and **1* variants, respectively. Additional studies are necessary to determine if the amino acid identities at these positions impact the catalytic activities of UGT1A8–UGT1A10 as was observed for UGT1A7. Although our study indicated that amino acid variation at these positions had no

effect on substrate specificity, it is possible that their interaction with other unique amino acids in the amino terminal domains of these enzymes helps to determine their subtle differences in substrate specificity. UGT1A8 was reported to be most active towards 10- and 11-OH-B(a)P, whereas UGT1A10 was most active towards 11- and 12-OH-B(a)P (Mojarrabi & Mackenzie, 1998). In the present study, UGT1A7 was most active towards 7-OH-B(a)P, followed in order by 3-OH, 9-OH, 8-OH-B(a)P and B(a)P-7,8-dihydrodiol. These data are consistent with the report of Strassburg et al. (1998) who found more than 10-fold higher UGT1A7 activity towards 7-OH-B(a)P compared to 8-OH-B(a)P.

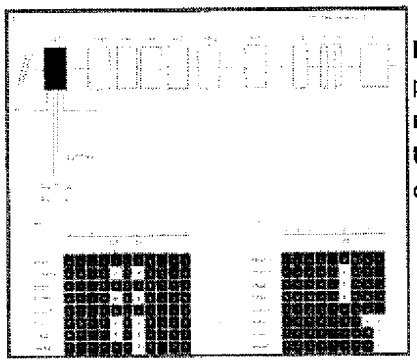


Fig. 8. Alignment with other members of the UGT1A isoenzymes. (a) Showing the partial *UGT1A* gene cluster and presents the location of the newly found missense mutations in the UGT1A7 first exon. Homology at regions of the protein presenting the new missense mutations are presented for UGT1A7 of lower species and among closely related UGT1A family members, at positions 129, 131 (b) and 208 (c).

[Help with image viewing]
[Email Jumpstart To Image]

UGTs were first described as membrane-bound proteins of the liver, however, recent findings now clearly show that extrahepatic tissues present a wide expression of these enzymes. Moreover, specific UGT1A proteins are shown to be particularly abundant in tissues other than the liver (Strassburg et al., 1997a,b, 1998;Hum et al., 1999). UGT1A7 has been described previously as an extrahepatic form with no detectable expression in the liver (Strassburg et al., 1997b). Our data confirm the absence of a UGT1A7 transcript in human liver and further show its expression in human lung. The expression of UGT1A7 in lung is particularly interesting since B(a)P and other polycyclic aromatic hydrocarbons act as carcinogens in this tissue. Several observations support a protective role of glucuronidation against B(a)P-induced genotoxicity (Vienneau et al., 1995;Kim & Wells, 1996;Kim et al., 1997). However, the relevance of our findings for understanding molecular and genetic factors involved in protection of human lung against carcinogenic polycyclic aromatic hydrocarbon exposures remains to be established.

Numerous studies suggest inter-individual variability in glucuronic acid conjugation in humans (Yue et al., 1989;Kalow, 1991;Patel et al., 1992;Rivory et al., 1997). Despite the fact that these variations might be due to changes at the expression level, the presence of genetic alterations in a specific UGT may certainly be an additional explanation. Genetic polymorphisms in the DME enzymes have been successfully linked to distinct phenotypes in the population. In addition, the implication in the disposition of drugs and their impact on one's susceptibility to specific diseases including cancer are well demonstrated for P450 enzymes and other phase II DMEs such as *GST* and *NAT* genes (Gonzalez, 1997;Ingelman-Sundberg, 1998;Nebert et al., 1999;Taningher et al., 1999). Based on the in-vitro and population studies presented herein, an important proportion of the population are homozygous carriers of the allele *UGT1A7*3* and appear to present much lower catalytic activity compared to the other genotypes. Additional studies are needed to fully address the biological consequences of constitutively altered UGT1A7 proteins, such as those presented in this study. Finally, the present findings support that considerable structural heterogeneity exists at the UGT1A loci more specifically at the *UGT1A7* gene. The identification of functional polymorphism in UGT proteins certainly constitutes an important step towards the understanding of inter-individual variation in the glucuronidation metabolic pathway, their pharmacological and toxicological importance and their role in cancer susceptibility.

Acknowledgements

We gratefully thanks Drs Daphne Bell and Dan Haber from Massachusetts General Hospital Cancer Center and Harvard Medical School for providing us germline DNAs from unrelated individuals. We also thanks Dr Anil Menon for providing additional African-American germline DNA samples which were used in the SSCP analysis. We also thanks Dr Eric Lévesque for helpful discussion. The Medical Research Council of Canada (MRCC) (C.G.) supported this work.

References

1. Aithal G, Day C, Kesteven P, Daly A. Association of polymorphisms in the cytochrome P450 CYP2C9 with warfarin dose requirement and risk of bleeding complications. Lancet 1999; 353: 717–719. **ArticleLinker**| **Full Text**| **Bibliographic Links**| [Context Link]

2. Bélanger A, Hum DW, Beaulieu M, Lévesque É, Guillemette C, Tchernof A. *et al.* Characterization and regulation of UDP-glucuronosyltransferases in steroid target tissues. J Steroid Biochem Molec Biol 1998; 65: 301–310. [Context Link]

3. Bell D, Wahrer D, Kang D, MacMahon M, FitzGerald M, Ishioka C. *et al.* Common nonsense mutations in RAD52. Cancer Res 1999; 59: 3883–3888. **ArticleLinker**| **Bibliographic Links**| [Context Link]

4. Beutler E, Gelbart T, Demina A. Racial variability in the UDP-glucuronosyltransferase 1 promoter: a balanced polymorphism for regulation of bilirubin metabolism. Proc Natl Acad Sci 1998; 95: 8170–8174. **ArticleLinker**| **Bibliographic Links**| [Context Link]

5. Bosma PJ, Roy Chowdhury J, Huang T-J, Lahiri P, Oude Elferink RPJ, Van Es HHG. *et al.* Mechanisms of inherited deficiencies of multiple UDP-glucuronosyltransferase isoforms in two patients with Crigler–Najjar syndrome, type 1. FASEB J 1992; 6: 2859–2863. **ArticleLinker**| **Bibliographic Links**| [Context Link]

6. Bosma P, Chowdhury J, Jansen P. Genetic inheritance of Gilbert's syndrome. Lancet 1995; 346: 314–315. **ArticleLinker**| **Full Text**| **Bibliographic Links**| [Context Link]

7. Cargill M, Altshuler D, Ireland J, Sklar P, Ardlie K, Patil N. *et al.* Characterization of single-nucleotide polymorphisms in coding regions of human genes. Nature Genet 1999; 22: 231–238. **ArticleLinker**| **Bibliographic Links**| [Context Link]

8. Chou Q, Russell M, Birch D, Raymond J, Bloch W. Prevention of pre-PCR mis-priming and primer dimerization improves low-copy-number amplifications. Nucl Acids Res 1992; 20: 1717–1723. **ArticleLinker**| **Full Text**| **Bibliographic Links**| [Context Link]

9. Ciotti M, Marrone A, Potter C, Owens IS. Genetic polymorphism in the human UGT1A6 UDP-glucuronosyltransferase: pharmacological implications. Pharmacogenetics 1997; 7: 485–495. **ArticleLinker**| **Bibliographic Links**| [Context Link]

10. Ciotti M, Basu N, Brangi M, Owens I. Glucuronidation of 7-ethyl-10-hydroxycamptothecin (SN-38) by the human UDP-glucuronosyltransferases encoded at the UGT1 locus. Biochem Biophys Res Commun 1999; 260: 199–202. **ArticleLinker**| **Full Text**| **Bibliographic Links**| [Context Link]

11. Coffman BL, King CD, Rios GR, Tephly TR. The glucuronidation of opioids, other xenobiotics, and androgens by human UGT2B7Y (268) and UGT2B7H (268). Drug Metab Disp 1998; 26: 73–77. **ArticleLinker**| **Bibliographic Links**| [Context Link]

12. Dutton GJ. *Glucuronidation of drugs and other compounds.* Boca Raton, FL: CRC Press; 1980. [Context Link]

13. Gonzalez FJ. The role of carcinogen-metabolizing enzyme polymorphisms in cancer susceptibility. Reprod Toxicol 1997; 11: 397–412. **ArticleLinker**| **Full Text**| **Bibliographic Links**| [Context Link]

14. Grove A, Kessler F, Metz R, Ritter J. Identification of a rat oltipraz-inducible UDP-glucuronosyltransferase (UGT1A7) with activity towards benzo(a)pyrene-7,8-dihydrodiol. J Biol Chem 1997; 272: 1621–1627. **ArticleLinker**| **Bibliographic Links**| [Context Link]

15. Guillemette C, Millikan R, Newman B, Housman D. Genetic polymorphisms in UGT1A1 and association with breast cancer among African Americans. Cancer Res 2000; 60: 950–956. [Context Link]

16. Halushka M, Fan J, Bentley K, Hsie L, Shen N, Weder A. *et al.* Patterns of single-nucleotide polymorphisms in candidate genes for blood-pressure homeostasis. Nature Genet 1999; 22: 239–247. **ArticleLinker**| **Bibliographic Links**| [Context Link]

17. Hum DW, Bélanger A, Lévesque E, Barbier O, Beaulieu M, Albert A. *et al.* Characterization of UDP-glucuronosyltransferases active on steroid hormones. J Steroid Biochem Mol Biol 1999; 65: 413–423. [Context Link]

18. Ingelman-Sundberg M. Functional consequences of polymorphism of xenobiotic metabolising enzymes. Toxicol Lett 1998; 102–103: 155–160. **ArticleLinker**| **Full Text**| **Bibliographic Links**| [Context Link]

19. Iyer L. Inherited variations in drug-metabolizing enzymes: significance in clinical oncology. Mol Diagn 1999; 4: 327–333. **ArticleLinker**| **Bibliographic Links**| [Context Link]

20. Kalow W. Interethnic variation of drug metabolism. Tips 1991; 12: 102–106. [Context Link]

21. Kim PM, Wells PG. Genoprotection by UDP-glucuronosyltransferases in peroxidase-dependent, reactive oxygen species-mediated micronucleus initiation by the carcinogens 4-(methylnitrosamino)-1-(3-pyridyl)-1-butanone and benzo[a]pyrene. Cancer Res 1996; 56: 1526–1532. **ArticleLinker**| **Bibliographic Links**| [Context Link]

22. Kim PM, Winn LM, Parman T, Wells PG. UDP-glucuronosyltransferase-mediated protection against in vitro DNA oxidation and micronucleus formation initiated by phenytoin and its embryotoxic metabolite 5-(p-hydroxyphenyl)-5-phenylhydantoin. J Pharmacol Exp Ther 1997; 280: 200–209. [Context Link]

23. Lévesque É, Beaulieu M, Green MD, Tephly TR, Bélanger A, Hum DW. Isolation and characterization of UGT2B15 (Y85): a UDP-glucuronosyltransferase encoded by a polymorphic gene. Pharmacogenetics 1997; 7: 317–325. **ArticleLinker**| **Bibliographic Links**| [Context Link]

24. Lévesque É, Beaulieu M, Hum DW, Bélanger A. Characterization and substrate specificity of UGT2B4 (E458): a UDP-glucuronosyltransferase encoded by a polymorphic gene. Pharmacogenetics 1999; 9: 206–217. **ArticleLinker**| [Context Link]

25. Mackenzie PI, Owens IS, Burchell B, Bock KW, Bairoch A, Bélanger A. *et al.* The UDP glycosyltransferase gene superfamily: recommended nomenclature update based on evolutionary divergence. Pharmacogenetics 1997; 7: 255–269. **ArticleLinker**| **Bibliographic Links**| [Context Link]

26. Mojarrabi B, Mackenzie P. Characterization of two UDP glucuronosyltransferases that are predominantly expressed in human colon. Biochem Biophys Res Commun 1998; 247: 704–709. **ArticleLinker**| **Full Text**| **Bibliographic Links**| [Context Link]

27. Monaghan G, Ryan M, Seddon R, Hume R, Burchell B. Genetic variation in bilirubin UDP-glucuronosyltransferase gene promoter and Gilbert's syndrome. Lancet 1996; 347: 578–581. **ArticleLinker**| **Full Text**| **Bibliographic Links**| [Context Link]

28. Nebert D, Ingelman-Sundberg M, Daly A. Genetic epidemiology of environmental toxicity and cancer susceptibility: human allelic polymorphisms in drug-metabolizing enzyme genes, their functional importance, and nomenclature issues. Drug Metab Rev 1999; 31: 467–487. **ArticleLinker**| **Bibliographic Links**| [Context Link]

29. Owens IS, Ritter JK. Gene structure at the human UGT1 locus creates diversity in isozymes structure, substrate specificity, and regulation. Prog Nucleic Acids Res 1995; 51: 306–338. [Context Link]

30. Patel M, Tang BK, Kalow W. Variability of acetaminophen metabolism in Caucasians and Orientals [see comments]. Pharmacogenetics 1992; 2: 38–45. **ArticleLinker**| **Bibliographic Links**| [Context Link]

31. Pillot T, Ouzzine M, Fournel-Gigleux S, Lafaurie C, Radominska A, Lester R. *et al.* Purification and characterization of a catalytically active human liver UDP-glucuronosyltransferase expressed as a fusion protein in *E. coli*. Biochem Biophys Res Commun 1993; 196: 473–479. **ArticleLinker**| **Full Text**| **Bibliographic Links**| [Context Link]

32. Ritter JK, Kessler F, Thompson M, Grove A, Auyeung D, Fisher R. Expression and inducibility of the human bilirubin UDP-glucuronosyltransferase UGT1A1 in liver and cultured primary hepatocytes: evidence for both genetic and environmental influences. Hepatology 1999; 30: 476–484. **ArticleLinker**| **Bibliographic Links**| [Context Link]

33. Ritter JK, Chen F, Sheen YY, Lubet RA, Owens IS. Two human liver cDNAs encode UDP-glucuronosyltransferases with 2 log differences in activity toward parallel substrates including hyodeoxycholic acid and certain estrogen derivatives. Biochemistry 1992a; 31: 3409–3414. [Context Link]

34. Ritter JK, Chen F, Sheen YY, Tran HM, Kimura S, Yeatman MT, Owens IS. A novel complex locus UGT1 encodes human bilirubin, phenol, and other UDP-glucuronosyltransferase isozymes with identical carboxyl termini. J Biol Chem 1992b; 267: 3257–3261. [Context Link]

35. Ritter JK, Yeatman MT, Kaiser C, Gridelli B, Owens IS. A phenylalanine codon deletion at the UGT1 gene complex locus of a Crigler-Najjar type I patient generates a pH-sensitive bilirubin UDP- glucuronosyltransferase. J Biol Chem 1993; 268: 23573–23579. **ArticleLinker**| **Bibliographic Links**| [Context Link]

36. Rivory L, Haaz M, Canal P, Lokiec F, Armand J, Robert J. Pharmacokinetic interrelationships of irinotecan (CPT-11) and its three major plasma metabolites in patients enrolled in phase I/II trials. Clin Cancer Res 1997; 3: 1261–1266. **ArticleLinker**| **Bibliographic Links**| [Context Link]

37. Smith P, Krohn R, Hermanson G, Mallia A, Gartner F, Provenzano M. *et al.* Measurement of protein using bicinchoninic acid. Anal Biochem 1985; 150: 76–85. **ArticleLinker**| **Full Text**| **Bibliographic Links**| [Context Link]

38. Strassburg CP, Manns MP, Tukey RH. Differential down-regulation of the UDP-glucuronosyltransferase 1A locus is an early event in human liver and biliary cancer. Cancer Res 1997a; 57: 2979–2985. [Context Link]

39. Strassburg CP, Oldhafer K, Manns MP, Tukey RH. Differential expression of the UGT1A locus in human liver, biliary, and gastric tissue: identification of UGT1A7 and UGT1A10 transcripts in extrahepatic tissue. Mol Pharmacol 1997b; 52: 212–220. [Context Link]

40. Strassburg CP, Mann MP, Tukey RH. Expression of the UDP-glucuronosyltransferase 1A locus in human colon. J Biol Chem 1998; 273: 8719–8726. **ArticleLinker**| **Bibliographic Links**| [Context Link]

41. Taningher M, Malacarne D, Izzotti A, Ugolini D, Parodi S. Drug metabolism polymorphisms as modulators of cancer susceptibility. Mutat Res 1999; 436: 227–261. **ArticleLinker**| **Bibliographic Links**| [Context Link]

42. Vienneau DS, DeBoni U, Wells PG. Potential genoprotective role for UDP-glucuronosyltransferases in chemical carcinogenesis: initiation of micronuclei by benzo(a)pyrene and benzo(e)pyrene in UDP-glucuronosyltransferase-deficient cultured rat skin fibroblasts. Cancer Res 1995; 55: 1045–1051. **ArticleLinker**| **Bibliographic Links**| [Context Link]

43. AT, Guillemette C, Cheung CL, Housman DE, Lieber CM. Carbon nanotube based DNA sequence determination and haplotyping in kilobase-size fragments, *Nature Biotech* in press. [Context Link]

44. Yue QY, Svensson JO, Alm C, Sjoqvist F, Sawe J. Interindividual and interethnic differences in the demethylation and glucuronidation of codeine. Br J Clin Pharmacol 1989; 28: 629–637. **ArticleLinker**| **Bibliographic Links**| [Context Link]

Keywords: glucuronidation; drug metabolism; genetic polymorphism; UGT1A7; benzopyrene

Copyright (c) 2000-2008 Ovid Technologies, Inc.
Version: OvidSP_UI02.00.02.101, SourceID 37332